Journal of Biomedical Optics

SPIEDigitalLibrary.org/jbo

Classification of reflected signals from cavitated tooth surfaces using an artificial intelligence technique incorporating a fiber optic displacement sensor

Husna Abdul Rahman
Sulaiman Wadi Harun
Hamzah Arof
Ninik Irawati
Ismail Musirin
Fatimah Ibrahim
Harith Ahmad

SPIE

Classification of reflected signals from cavitated tooth surfaces using an artificial intelligence technique incorporating a fiber optic displacement sensor

Husna Abdul Rahman,[a,b,c,*] Sulaiman Wadi Harun,[a,b] Hamzah Arof,[a] Ninik Irawati,[b] Ismail Musirin,[c] Fatimah Ibrahim,[d] and Harith Ahmad[b]
[a]University of Malaya, Department of Electrical Engineering, Faculty of Engineering, Kuala Lumpur 50603, Malaysia
[b]University of Malaya, Photonics Research Centre, Department of Physics, Faculty of Science, Kuala Lumpur 50603, Malaysia
[c]Universiti Teknologi MARA (UiTM), Faculty of Electrical Engineering, Shah Alam 40450, Malaysia
[d]University of Malaya, Medical Informatics and Biological Micro-electro-mechanical Systems Specialized Laboratory, Department of Biomedical Engineering, Faculty of Engineering, Kuala Lumpur 50603, Malaysia

Abstract. An enhanced dental cavity diameter measurement mechanism using an intensity-modulated fiber optic displacement sensor (FODS) scanning and imaging system, fuzzy logic as well as a single-layer perceptron (SLP) neural network, is presented. The SLP network was employed for the classification of the reflected signals, which were obtained from the surfaces of teeth samples and captured using FODS. Two features were used for the classification of the reflected signals with one of them being the output of a fuzzy logic. The test results showed that the combined fuzzy logic and SLP network methodology contributed to a 100% classification accuracy of the network. The high-classification accuracy significantly demonstrates the suitability of the proposed features and classification using SLP networks for classifying the reflected signals from teeth surfaces, enabling the sensor to accurately measure small diameters of tooth cavity of up to 0.6 mm. The method remains simple enough to allow its easy integration in existing dental restoration support systems. [DOI: 10.1117/1.JBO.19.5.057009]

Keywords: fiber optic displacement sensor; scanning and imaging system; dental cavity; classification; single-layer perceptron neural network; fuzzy logic.

Paper 140001R received Jan. 2, 2014; revised manuscript received Mar. 10, 2014; accepted for publication Apr. 7, 2014; published online May 19, 2014.

1 Introduction

The numerous breakthroughs in photonics that have taken place over the last 50 years gave rise to many other applications in health care. Scientific and technological advances have led to the improvement in dental diagnostic tools. However, the pace of photonics applications in clinical dentistry has been significantly slower than in clinical medicine. The application of optical technology in dentistry is well worth exploring due to its excellent potential in providing information noninvasively, and the ability to induce localized and specific structure changes. Hence, it is of great interest to extend the success of fiber optic displacement sensor (FODS) employment[1–6] to several dental applications. Previously, the capability of the FODS in discriminating between different teeth surfaces was demonstrated,[7] employing both of the fiber optic coupler and concentric fiber optic bundle as the probe. Such results are useful as guidelines for tooth surface-related researches such as tooth surface profiling, colorimetric analysis in dentistry, and measurement of tooth surface roughness.[8,9]

In dentistry, a successful restorative procedure depends strongly on the precise mapping of the shape of dental cavities. However, the impression material might suffer from shape and size deformity during the course of mapping, copying, and storage, leading to defects in the process. Furthermore, this technique requires skilled workers, i.e., dental technicians, to be able to fabricate precise restorations from the casts obtained by impression making. In light of these significant constraints there arises a need for a system and method for the digitization of the tooth surfaces, which can be used for the restorations in a dental laboratory.

Several research groups have been working to develop noncontact optical-based technologies for dental restoration to reduce possible errors during the traditional impressional methods; but most of them are still under the clinical testing stages. One particular scanning device that has been commercialized uses the basic principles of confocal microscopy and active triangulation technique.[10–12] An illumination beam on the surface of the target object is produced by a blue light-emitting diode and a focusing system is used to focus the observation beam onto the image sensor. Image stabilization systems are included in the system and a short-scanning time of less than a minute is required to scan the surface of a tooth. Despite the advantages, the tooth surface needs to be coated with opportune powders before each scanning stage. Another commercialized technique utilizes a parallel confocal imaging technique. This technique does not require coatings on the tooth surface due to the inclusion of a color wheel inside the acquisition unit, which results in a larger scanner head compared with other systems.[13,14] Each of the foregoing systems suffer the drawback in which expensive specialized devices are required, hence hindering the widespread use of the systems especially in developing countries.

*Address all correspondence to: Husna Abdul Rahman, E-mail: husna_ar@yahoo.com

The recent findings involve the imaging of cavities on various teeth surfaces using FODS. Preliminary results were discussed, and measurements of the diameter of the cavities which were represented by drilled holes were performed.[15] The proposed sensor in Ref. 15 makes use of the measured reflected signal taken along the same axis of a cavitated and an uncavitated tooth surface and makes use of the difference in the reflected signal between them to decide on the cavity region. However, several drawbacks have been identified, such as the inability of the sensor to correctly measure the diameter of the cavity due to experimental inconsistencies and laser source error. HeNe lasers experience both periodic and random fluctuations. Periodic fluctuations occur due to the ripple of the discharge current caused by an insufficiently filtered power supply. On the other hand, the spikes of the power supply, instabilities of the gas discharge, and vibrations of the resonator mirrors are the cause for random fluctuations.[16] This problem is more apparent in smaller sized cavities, particularly those smaller than the diameter of the laser source. This results from the increase in the occurrence of signal disparity, which is due to the partial illumination of the laser on the cavity region leading to false estimation of the cavity diameter. Moreover, it is generally neither practical nor feasible within a real clinical setting to obtain the measured reflected signal from the uncavitated tooth surface prior to the cavitation process, hence hindering the prospect for commercialization.

On these grounds, we propose an approach to classify reflected signals as either "reflected signals of the cavitated region" (RSC) or "reflected signals of the surrounding uncavitated region" (RSSU) for the purpose of measurement of cavity diameter. An enhanced dental cavity imaging mechanism by using intensity modulated FODS scanning and imaging system as well as a single-layer perceptron (SLP) neural network is proposed. The SLP network is fed with two input features; one of them being the output of a fuzzy logic. The application of an SLP network excludes partial membership of the reflected signals resulting from partial illumination of laser on the cavity region. The ability of the network to produce accurate results independent of the tooth surface type and the measured reflected signals prior to the cavitation process is explored.

2 Classification Methodology

In order to perform the classification of the reflected signals, the actions to be taken will include four main steps, starting with the image acquisition, cavity localization, feature extraction, fuzzy logic, and end with the classification using SLP network at the final step (Fig. 1). In this research, a total of five images were captured from various teeth samples by using the FODS imaging technique[15] at a resolution of 0.1-mm gap distance between the reflected signals.

2.1 *Image Acquisition*

A scanning system was constructed as shown in Fig. 2. The system consists of a light source, mechanical chopper, fiber

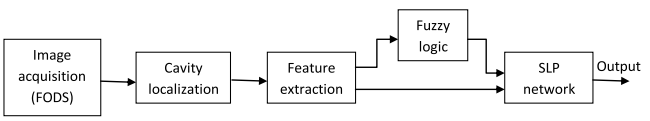

Fig. 1 Research design stages.

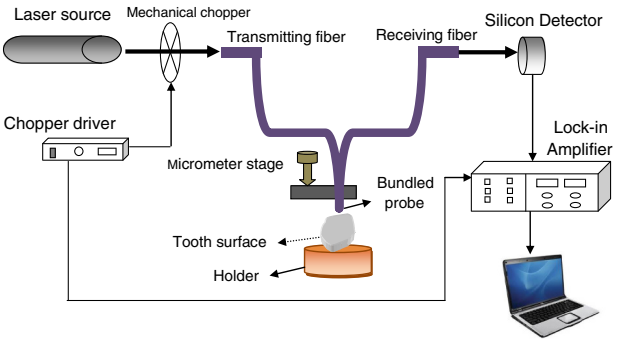

Fig. 2 Set-up for the imaging of tooth cavity using fiber optic displacement sensor.

optic probe, five teeth samples (consisting three of the acrylic teeth surfaces and two of the canine teeth surfaces), a silicon photodetector, lock-in amplifier, and computer. The two canine teeth surfaces were extracted and stored at room temperature 1 week prior to the experiments. In addition, three acrylic resin teeth surfaces (GC Permacryl, Tokyo, Japan) were also used as reflecting surfaces. Flaws were introduced in each of the teeth samples by drilling holes of various diameters that mimic dental cavities. The fiber optic probe was made of two 2-m-long PMMA (polymethyl methacrylate) consisting of one transmitting fiber of 1 mm in diameter and 16 receiving fibers of 0.25 mm in diameter, numerical aperture of 0.5, core refractive index of 1.492, and cladding refractive index of 1.402. A red He-Ne laser ($\lambda = 633$ nm) was used as the light source with an average output power of 5.5 mW, beam diameter of 0.80 mm and beam divergence of 1.01 mRads. The photodetector used was a high-speed silicon photodiode with an optical response extending from 400 to 1100 nm, making it compatible with a wide range of visible light including the 633-nm visible red He-Ne laser used in this set-up. The light source was modulated externally by a chopper with a frequency of 113 Hz as to avoid the harmonics from the line frequency ranging from 50 to 60 Hz. The modulated light source was used in conjunction with a lock-in amplifier to reduce the dc drift and interference of ambient stray light.

The displacement of the fiber optic probe was achieved by mounting it on a micrometer translation stage, which was rigidly attached to a vibration free table. Light from the fiber optic transmitter was coupled into the transmitting fiber. The signal from the receiving fiber was measured by moving the probe away from the zero point, where the reflective surface of the tooth and the probe were in close contact. The signal from the silicon photodetector was converted to voltage and was measured by a lock-in amplifier and computer via RS232 using a Delphi software. The surrounding uncavitated surface of the five teeth surfaces was used consecutively as the reflecting target whilst measuring the output intensity by changing the position of the fiber optic probe axially (z-axis) from 0 to 4.7 mm in a step of 0.05 mm.

The probe was consequently fixed within the linear range of the displacement curve and the intensity of the collected light as a function of lateral movement (x and y axes) of the tooth surface was recorded while being maintained in perpendicular and constant in axial position (z axis). The experiment was carried out with minimum successive steps of 0.1 mm for each of the tooth surface. The methodology for diameter quantification of the cavity in Ref. 15 was repeated for the acrylic teeth surfaces,

where the differences in the reflected light between the cavitated and uncavitated tooth regions were exploited. Then, the proposed combination methodology of FODS, fuzzy logic, and SLP network was applied onto the same set of acrylic teeth surfaces together with a new set of canine teeth surfaces. During the experiment, the temperature was kept constant at 25°C, and the error due to this temperature variation is negligible.

2.2 *Cavity Localization and Feature Extraction*

The exact location of the cavity in an image is needed to ensure a robust and accurate feature extraction. The goal of the cavity localization is finding a region in an image as a cavity candidate whose shape resembles the shape that contains the most important information of a cavity. The change in amplitude between subsequent values in a stream of reflected signals through the center of the cavity, henceforth referred to as the "cavitated axis" was measured. The change occurring between the current and the previous reflected signal is referred to as α, whereas the change occurring between the current and the next reflected signal is referred to as β. Both parameters can take up either a positive, negative, or zero value indicating a higher, lower, or identical subsequent value, respectively. The starting of the cavity region is indicated by either a zero or negative α followed by either a positive or zero β. Meanwhile, the ending of the cavity region is indicated by a negative α followed by either a positive or zero β. The value of the constant reference signal was determined during the calibration process and is higher than all the reflected signal values along the cavitated axis. The constant reference signals for new types of teeth surfaces, $\mathrm{Ref}_{\mathrm{new}}$ was selected such that the difference between the lowest reflected signals within the cavity region with the constant reference signal is the same as that of the calibrated teeth surface, $\mathrm{Diff}_{\mathrm{c}}$, as defined in Eqs. (1) and (2).

$$\mathrm{Diff}_{\mathrm{c}} = \mathrm{Ref}_{\mathrm{c}} - \mathrm{MRC}_{\mathrm{c}}, \tag{1}$$

$$\mathrm{Ref}_{\mathrm{new}} = \mathrm{Diff}_{\mathrm{c}} + \mathrm{MRC}_{\mathrm{new}}, \tag{2}$$

where $\mathrm{Ref}_{\mathrm{c}}$ is the constant reference signal of a calibrated tooth surface, $\mathrm{MRC}_{\mathrm{c}}$ is the lowest reflected signal within the cavity region of a calibrated tooth surface, and $\mathrm{MRC}_{\mathrm{new}}$ is the lowest reflected signal within the cavity region of a new tooth surface.

The selected cavity region is then refined after filtering out the reflected signals that are higher than the constant reference signal.

After cavity localization, the next step is to perform the feature extraction. The extracted features will provide useful information for the classification of reflected signals as either RSC or RSSU. Several variables were used for the feature extraction process, which are as follows:

γ: The amplitude difference between the reflected signals along the cavitated axis with a constant reference signal.

β: The change occurring between the current and the next reflected signal along the cavitated axis.

$\mathrm{D}_{\mathrm{min}}$: The distance between the locations of the current reflected signal with the minimum reflected signal within a localized cavity region.

Here, the first feature is based on γ, whereby positive γ signifies a higher reference signal, whereas a negative γ signifies a lower reference signal. A higher γ magnitude is an indication of a larger difference gap between the reflected signal and the constant reference signal. The second feature (F2) is the output of a fuzzy logic, derived from γ, β, and $\mathrm{D}_{\mathrm{min}}$.

2.2.1 *Fuzzy logic*

The output value of the fuzzy logic ranges from 0 to 10. The objective in this stage is to provide the second input feature to the SLP network. Fuzzification layer in the input of the SLP network with several membership functions for each input (Table 1) was performed. Through a fuzzification interface, the matching degree of the crisp inputs, namely γ, β, and $\mathrm{D}_{\mathrm{min}}$ are calculated to a prespecified membership function consisting of the triangular-shaped function [Eq. (3)], trapezoidal-shaped function [Eq. (4)], and Gaussian function [Eq. (4)].

$$f(x) = \begin{cases} 0, & x < b_1 \\ \frac{x-b_1}{b_2-b_1}, & b_1 \le x \le b_2 \\ \frac{b_3-x}{b_3-b_2}, & b_2 \le x \le b_3 \\ 0, & x \ge b_3 \end{cases}, \tag{3}$$

$$f(x) = \begin{cases} 0, & x < a_1 \\ \frac{x-a_1}{a_2-a_1}, & a_1 \le x \le a_2 \\ 1, \ldots & a_2 \le x \le a_3 \\ \frac{a_4-x}{a_4-a_3}, & a_3 \le x \le a_4 \\ 0, & x \ge a_4 \end{cases}, \tag{4}$$

$$f(x) = e^{-\frac{(x-c)^2}{2\sigma^2}}. \tag{5}$$

The three numbers, b_1, b_2, and b_3, of the triangular-shaped membership function in Eq. (3) represent the three corners of a triangle. Similarly, the numbers a_1, a_2, a_3, and a_4 in Eq. (4) represent the four corners of a trapezoid in x-axis starting from the left bottom corner and going along the clockwise direction. $[\sigma, c]$ is the center and width of a Gaussian function.

The developed rules are as follows:

Table 1 The linguistic variables for each class.

Fuzzy system variable	Membership function	Type	Parameters
γ	Negative, Zero, Positive	Trapezoidal, Triangular, Trapezoidal	[−0.18 −0.18 0 0.01], [−0.02 0 0.02], [−0.01 0 0.7 0.7]
β	Negative, Zero, Positive	Trapezoidal, Triangular, Trapezoidal	[−0.2 −0.2 0 0.01], [−0.02 0 0.02], [−0.01 0 0.045 0.045]
$\mathrm{D}_{\mathrm{min}}$	Small, Large	Triangular, Triangular	[−0.01 0 0.012], [0.012 0.04 0.04]
Fuzzy output	Noncavity, Cavity	Gaussian, Gaussian	[2.4 0], [2.4 0]

1. If γ is negative then fuzzy output is noncavity.
2. If γ is zero then fuzzy output is noncavity.
3. If γ is positive and β is negative and D_{min} is small, then fuzzy output is cavity.
4. If γ is positive and β is negative and D_{min} is large, then fuzzy output is noncavity.
5. If γ is positive and β is positive and D_{min} is small, then fuzzy output is cavity.
6. If γ is positive and β is positive and D_{min} is large, then fuzzy output is noncavity.
7. If γ is positive and β is zero and D_{min} is small, then fuzzy output is cavity.

For the consequent part of the rules the implication operator of Mamdani was used.

2.3 *Application of the Neural Network Model*

An SLP network with hard-limit transfer function was used as the classifier. The hard-limit transfer function receives external inputs that have been appropriately weighted alongside an input of 1 from the bias. The hard-limit transfer function divides the input space into two regions and returns either a 0 or a 1.

Figure 3 shows the block diagram for the developed reflected signal classification architecture. In the block diagram, γ, the amplitude difference between the reflected signals along the cavitated axis with a constant reference signal was used as the input, cascaded with the fuzzy logic output to form the overall input data of the SLP network. The tooth surface region was assigned as the targeted output of the SLP network. Output 1 was assigned to the RSC class and output 0 to the RSSU class. The classification accuracy which is calculated as the ratio of the number of samples correctly classified to the total number of samples[17] is measured for each of the input data.

There are several reasons for using SLP instead of more complex artificial neural network (ANN) alternative models in this particular case. The SLP network is appealing due to its ability to generalize from its training vectors and learn from initially randomly distributed connections. Nevertheless, such a network is suited for cases with only two outputs and for the classification of linearly separable problems. SLP is preferred as they are fast and reliable networks for the problems they can solve and also involve simpler parameter adjustments.

3 Results and Discussions

Figure 4 shows the measured reflected signal taken along both the cavitated and uncavitated axis of the first acrylic tooth surface. The region of interest marked by the circle represents the localized cavity region. It demonstrates the clear difference in the reflected signal between them. In Ref. 15, the diameter of the cavity was measured based on the total lateral displacements starting from the first occurrence of disparity in the reflected signals and ends with the coincidence of the signals. Taking into account the distance of 0.1 mm for each displacement, the diameter is measured to be 2.8 mm, which is inconsistent with the micrometer measurement of 0.9 mm. It is apparent that this approach does not work for smaller cavity diameters, particularly for those <1 mm, as it is in close proximity to the 0.8-mm beam width of the laser source.

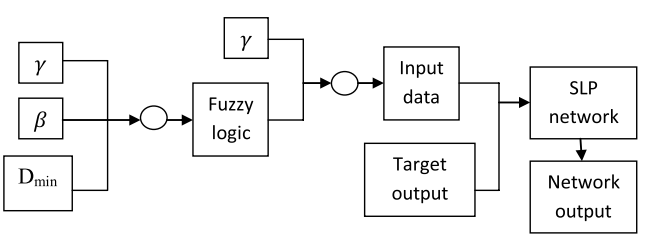

Fig. 3 Architecture for the classification of the reflected signal from cavitated tooth surface.

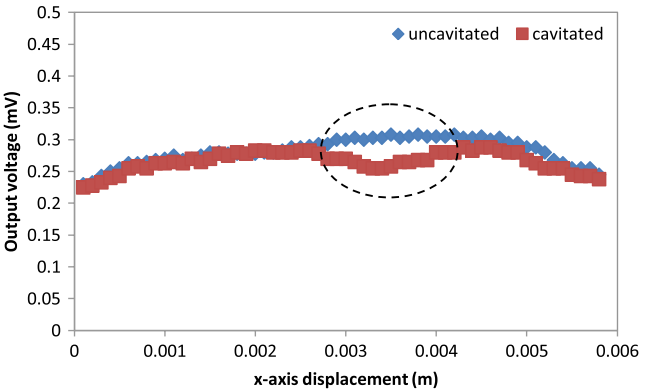

Fig. 4 Variation of output voltage against position along the cavitated and uncavitated axis of the first acrylic tooth surface.

The SLP network that has been proposed to address this issue was initially applied to the cavitated axis of the first acrylic tooth surface for the calibration process. Here, we attempt to repeat the analysis of the acrylic tooth surfaces again using the constant reference signal as a comparison. Figure 5 shows the measured reflected signal taken along the cavitated axis of the first acrylic tooth and a constant reference signal, consisting of 34 reflected signals each within the localized cavity region. Figure 6 shows the classification groups of RSC and RSSU. As can be seen, the separation groups are linearly separable hence confirming the use of an SLP network. Ten points were used for artificial neural network training and the rest were used for testing the system. Nine reflected signals were correctly classified as RSC yielding a cavity diameter of 0.9 mm. 100% of the data were accurately classified with the employment of SLP network.

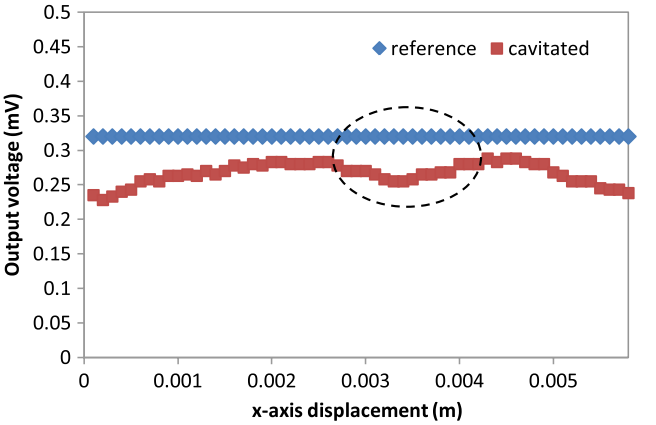

Fig. 5 Variation of output voltage against position along the cavitated axis of the first acrylic tooth surface and a constant reference signal.

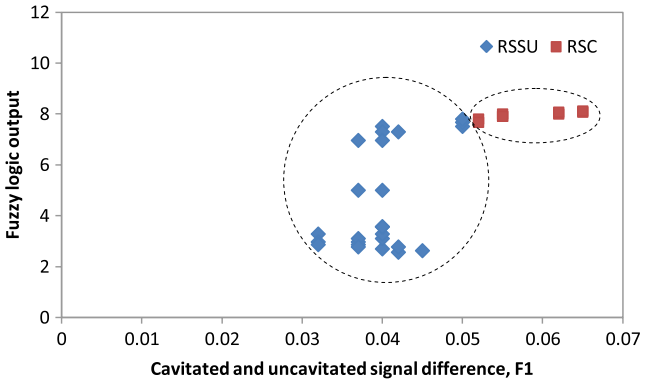

Fig. 6 The reflected signals of the cavitated region (RSC) and reflected signals of the surrounding uncavitated region (RSSU) classification group from the first acrylic tooth surface based on the two features, amplitude difference between the reflected signals along the cavitated axis and the constant reference signal, (F1) and fuzzy logic output based on γ, β, and D_{min}, (F2).

Figures 7(a) and 7(b) show the measured reflected signal taken along both the cavitated and uncavitated axes of the second and third acrylic tooth surface, respectively. The methodology for the tooth cavity measurement explained in Ref. 15 yielded a cavity diameter of 1.9 and 1.6 mm, respectively. Figures 8(a) and 8(b) show the measured reflected signal taken along the cavitated axis of the second and third acrylic

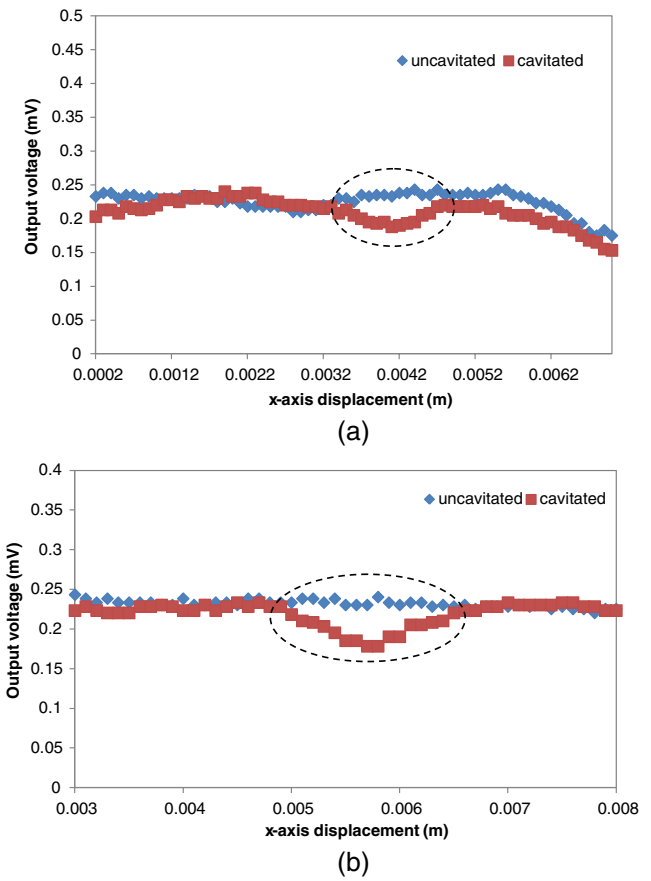

Fig. 7 Variation of output voltage against position along the cavitated and uncavitated axis of the (a) second and (b) third acrylic tooth surface.

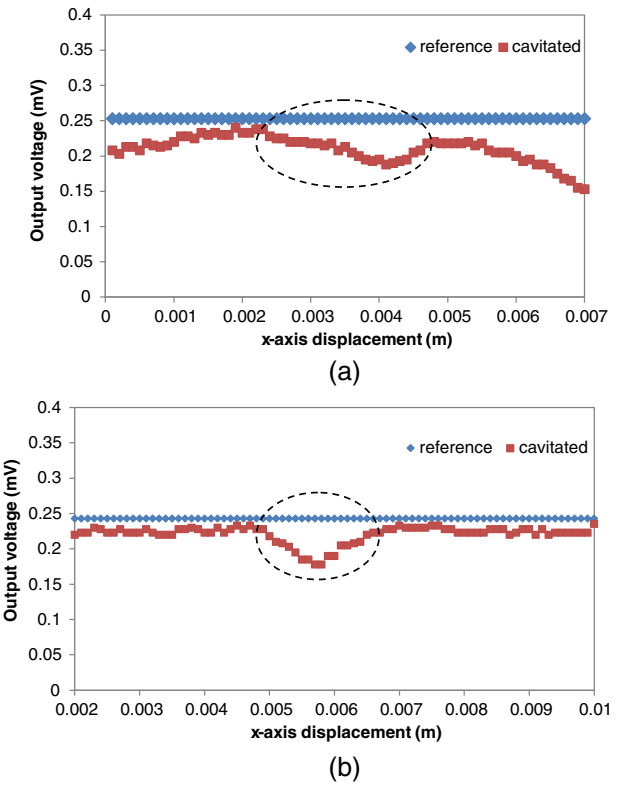

Fig. 8 Variation of output voltage against position along the cavitated axis of the (a) second and (b) third acrylic tooth surface and a constant reference signal.

tooth surface, respectively together with the constant reference signal. The two characteristics, F1 and F2 for each of the 20 and 16 reflected signals within the localized cavity region of the second and third acrylic tooth surface, respectively, were made as inputs to the trained SLP network. The testing results yielded a diameter of 0.8 and 0.6 mm for the second and third acrylic tooth surfaces, respectively, matching the one measured by the micrometer (100% data classification accuracy).

The process was repeated on a pair of cavitated canine teeth surfaces. Here, the reflected signals prior to the cavitation process were not measured beforehand. Since a new type of tooth surface is being used, a new calibration procedure has to be performed on the first canine tooth surface, involving the first step of measuring the cavity diameter of 0.9 mm using a micrometer.

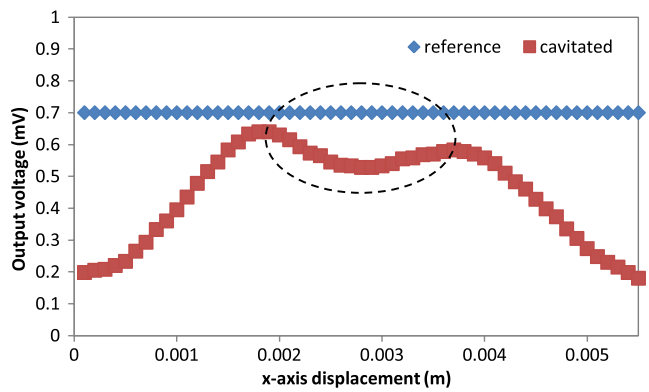

Fig. 9 Variation of output voltage against position along the cavitated axis of the first canine tooth surface and a constant reference signal.

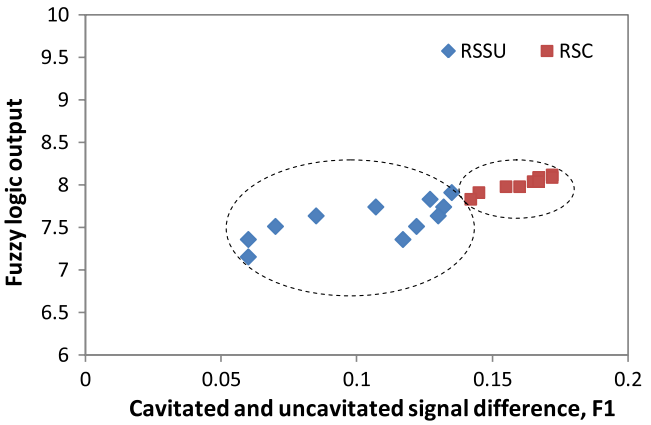

Fig. 10 The RSC and RSSU classification group from the first canine tooth surface based on the two features, amplitude difference between the reflected signals along the cavitated axis and the constant reference signal, (F1) and fuzzy logic output based on γ, β, and D_{min}, (F2).

The localized cavity region (consisting of a total of 23 reflected signals) was then determined as depicted in Fig. 9. Figure 10 illustrates the two linearly separable groups classified based on the two features, F1 and F2. Ten points were used for SLP network training and 13 were used for testing the system leading to a 100% of data classification accuracy.

Figure 11 shows the measured reflected signal taken along the cavitated axis of the second canine tooth surface and a constant reference signal The two characteristics for each of the 19 reflected signals within the localized cavity region were made as inputs to the trained SLP network and the testing results yielded a cavity diameter of 0.8 mm, which is exactly the same as the micrometer measurement. Again, the network provides 100% data classification accuracy.

Table 2 summarizes the diameter measurement of the cavity performed by using the combination of FODS, fuzzy logic, and SLP network. A wide gap difference with the actual cavity diameter (obtained through micrometer measurements) of 1.9, 1.1, and 1 mm for the first, second, and third acrylic sample, respectively, was obtained by merely using the FODS imaging system. The employment of fuzzy logic and SLP network into the FODS imaging system has bridged the gap for all five teeth

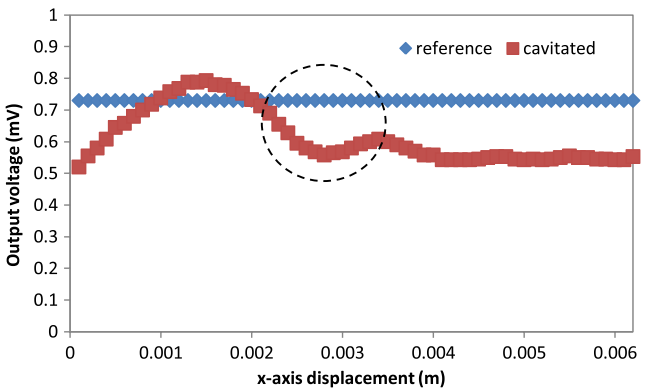

Fig. 11 Variation of output voltage against position along the cavitated axis of the second canine tooth surface and a constant reference signal.

Table 2 Diameter measurement of the cavity on the tooth surface using the fiber optic displacement sensor (FODS), fuzzy logic, single-layer perceptron (SLP) network and micrometer.

No	Type of tooth surface	FODS measurements (mm)	FODS measurements with fuzzy logic and SLP network (constant reference signal as comparison)	Micrometer measurements (mm)
1	Acrylic sample 1	2.8	0.9	0.9
2	Acrylic sample 2	1.9	0.8	0.8
3	Acrylic sample 3	1.6	0.6	0.6
4	Canine sample 1	—	0.9	0.9
5	Caninne sample 2	—	0.8	0.8

surfaces, evidently able to produce more accurate cavity diameter measurements.

The summary of the SLP network parameters for both of the acrylic and canine tooth surface is tabulated in Table 3. Both of the networks achieved a 100% classification rate by incorporating the HARDLIM and LEARNP as the transfer function and learning function, respectively. The transfer function used for the SLP network is HARDLIM, which returns either a 0 or a 1. Hence, only two outputs per neuron are permitted. Due to the different reflectivity of the acrylic tooth and canine tooth surfaces, different clusters are formed based on the input features, resulting in a total of four clusters altogether. Two different SLP network with different numerical value of parameters are needed to classify all the input into four clusters. The SLP network for the acrylic tooth surface utilized 10 training patterns using 63 numbers of epochs and 24 testing patterns. On the other hand, the SLP network for the canine tooth surface utilized 10 training patterns using 59 numbers of epochs and 13 testing patterns.

The sensor proves to be simple and easy to be implemented. However, in order to cater for higher resolution requirements, smaller displacements need to be applied, with more reflected signals for improved accuracy. Furthermore, the use of

Table 3 Summary of the SLP network parameters.

Parameters	Acrylic tooth surface	Canine tooth surface
Transfer function	HARDLIM	HARDLIM
Learning function	LEARNP	LEARNP
No. of training data	10	10
No. of testing data	24	13
No. of epochs	63	59
Classification (%)	100	100

picomotor actuators can significantly reduce the scanning time depending on the type used. Cavity measurements via two-dimensional analysis can also be implemented by using more powerful image processing and artificial intelligence techniques.

4 Conclusions

In conclusion, the enhanced FODS scanning and imaging system for tooth cavity detection proposed in this research was validated via a simple and controlled experiment, and the experiment results show that this improved method could accurately measure small diameters of tooth cavity of up to 0.6 mm. The tooth cavity is obtained by passing through three steps; the scanning and imaging by FODS, feature extraction using fuzzy logic, and the classification of reflected signals by SLP neural networks. The proposed approach has been trained and tested with known and unknown tooth cavity diameters, respectively, using constant reference signal for the comparison analysis. The test results showed that the proposed system provided accurate diameter calculation with a 100% success rate. The key point is using a low-cost device that can perform accurately as an expensive device and the fact that further enhancements can be made to the resolution without the need of any extra hardware proves to be valuable for potential consumers.

Acknowledgments

The authors are grateful to Dr. Suhaila Abdullah and Dr. Mohd Noor Fareezul Noor Shahidan for providing the human teeth samples used in this experiment. This work is financially supported by University of Malaya, Ministry of Higher Education High Impact Research (UM/HIR/MOHE/ENG/05).

References

1. H. A. Rahman et al., "Fiber-optic salinity sensor using fiber-optic displacement measurement with flat and concave mirror," *IEEE J. Sel. Top. Quantum Electron.* **18**(5), 1529–1533 (2012).
2. C. S. Lin and R. S. Chang, "Fiber optic displacement sensors for the measurement of a vibrating object," *Precis. Eng.* **16**(4), 302–306 (1994).
3. D. Sastikumar, G. Gobi, and B. Renganathan, "Determination of the thickness of a transparent plate using a reflective fiber optic displacement sensor," *Opt. Laser Technol.* **42**(6), 911–917 (2010).
4. S. Binu, V. Mahadevan Pillai, and N. Chandrasekaran, "Fibre optic displacement sensor for the measurement of amplitude and frequency of vibration," *Opt. Laser Technol.* **39**(8), 1537–1543 (2007).
5. S. Binu et al., "PMMA (polymethyl methacrylate) fiber optic probe as a noncontact liquid level sensor," *Microwave Opt. Technol. Lett.* **52**(9), 2114–2118 (2010).
6. H. Golnabi, "Mass measurement using an intensity-modulated optical fiber sensor," *Opt. Lasers Eng.* **38**(6), 537–548 (2002).
7. H. A. Rahman et al., "Fiber optic displacement sensor using multimode plastic fiber probe and tooth surface," *IEEE Sens. J.* **13**(1), 294–298 (2013).
8. H. A. Rahman et al., "Fiber optic displacement sensor for imaging of tooth surface roughness," *Measurement* **46**(1), 546–551 (2012).
9. H. A. Rahman et al., "Detection of stain formation on teeth by oral antiseptic solution using fiber optic displacement sensor," *Opt. Laser Technol.* **45**, 336–341 (2013).
10. M. Bradestini and W. H. Moermann, "Method and apparatus for the three dimensional registration and display of prepared teeth," U.S. Patent 4837732 (1989).
11. A. Schwotzer, "Measuring device and method that operates according to the basic principles of confocal microscopy," U.S. Patent 7679723 (2010).
12. V. Schmidt, "3D dental camera for recording surface structures of a measuring object by means of triangulation," U.S. Patent 2011/0242281 (2011).
13. N. S. Birnbaum et al., "3D digital scanners: a high-tech approach to more accurate dental impressions," *Inside Dent.* **5**(4), 70–74 (2009).
14. N. Babayoff and I. Glaser-Inbari, "Imaging a three-dimensional structure by confocal focussing an array of light beams," U.S. Patent 6697164 (2004).
15. H. A. Rahman et al., "Feasibility of fiber optic displacement sensor scanning system for imaging of dental cavity," *J. Biomed. Opt.* **17**(7), 071308 (2012).
16. W. Demtröder, *Laser Spectroscopy: Basic Concepts and Instrumentation*, Springer, Berlin (2003).
17. A. B. Sankar et al., "Effective enhancement of classification of respiratory states using feed forward back propagation neural networks," *Sadhana* **38**(3), 377–395 (2013).

Husna Abdul Rahman received her BEng (Hons) from Multimedia University, Malaysia, in 2002. Her MSc degree is from the University of Surrey, UK, in mobile communication system. She is currently pursuing her PhD in photonics at the University of Malaya, Malaysia. She is also a lecturer in the Faculty of Electrical Engineering, MARA University of Technology (UiTM), Malaysia.

Sulaiman Wadi Harun received his BE degree in electrical and electronics system engineering from Nagaoka University of Technology, Japan, in 1996, and MSc and PhD degrees in photonics from the University of Malaya in 2001 and 2004, respectively. Currently, he is a full professor in the Faculty of Engineering, University of Malaya. His research interests include fiber optic active and passive devices.

Hamzah Arof is a full professor in the Faculty of Engineering, University of Malaya.

Ninik Irawati is currently pursuing her master's degree in photonics at the University of Malaya, Malaysia.

Ismail Musirin is an associate professor in the Faculty of Electrical Engineering, University Teknologi MARA. His research interests are related to AI applications.

Fatimah Ibrahim is a full professor in the Faculty of Engineering, University of Malaya.

Harith Ahmad is a full professor in the Faculty of Science, University of Malaya.